

Abstract

Interpreting magnetotelluric (MT) data in regions with rugged topography and galvanic distortion poses significant challenges. Although advanced 3D MT inversion algorithms exist to address these issues, their adoption is limited by the complexities of multi-resolution adaptive meshes and solving inverse problems. This study presents our methodology for evaluating the effects of topography and distortion on MT data interpretation, utilizing a 3D

MT survey from the geothermal resource assessment project at the Northeast Carpathian Volcanic Arc in Northern Romania. The Baia Mare mining district, characterized by significant elevation changes and scattered near-surface conductive anomalies, serves as the study area. We compare the performance of the finite-difference ModEM code and the hybrid finite element DEVA3DMT software, assessing their ability to handle topographical

features and distortion correction. Our findings demonstrate the critical role of incorporating topography and distortion correction in the inversion workflow, highlighting issues such as near-surface conductivity anomalies and biased forward modeling results. This analysis emphasizes the importance of these factors in MT data interpretation and provides insights into the effectiveness of different inversion approaches.

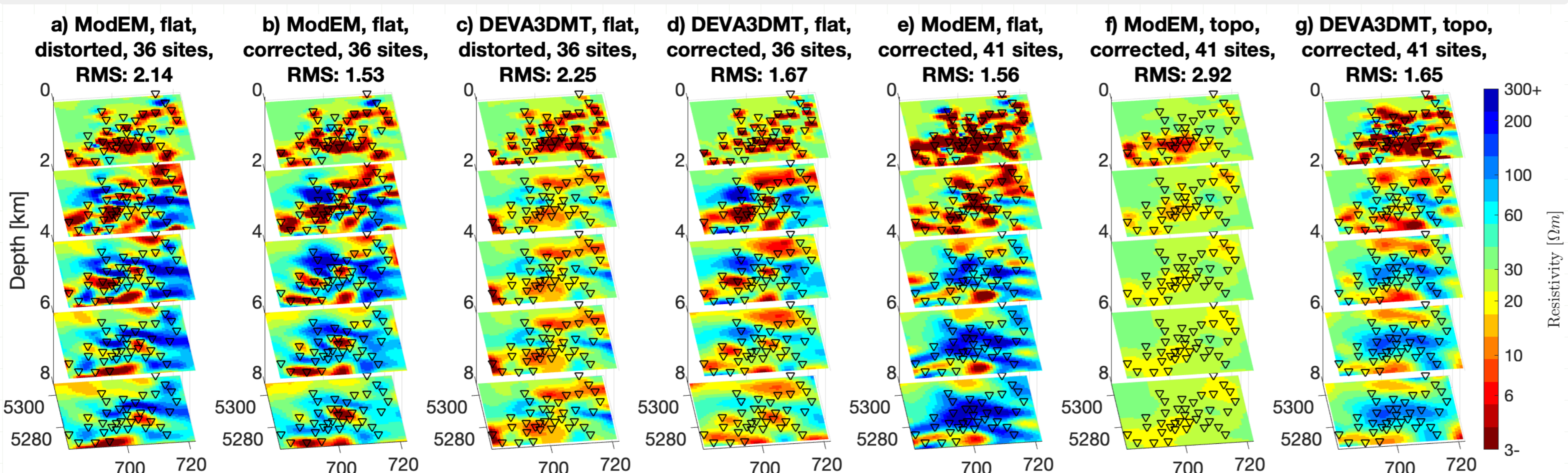


Figure 1: Resistivity models from ModEM and DEVA3DMT software are presented for various scenarios, with eight depth slices shown every 2 km below sea level. Panels (a) to (d) display results from 36 sites (8Hz to 16384s), using both original and distortion-corrected

data. DEVA3DMT also attempted to recover distortion parameters as part of the inversion. Panels (e) to (g) show results from 41 sites (36 MT and 5 pseudo-MT, 128Hz to 8192s), highlighting the impact of topography. Only distortion-corrected data

is used here. ModEM performs well with a flat model but struggles with topography due to a coarse model discretization, whereas DEVA3DMT effectively incorporates topography.

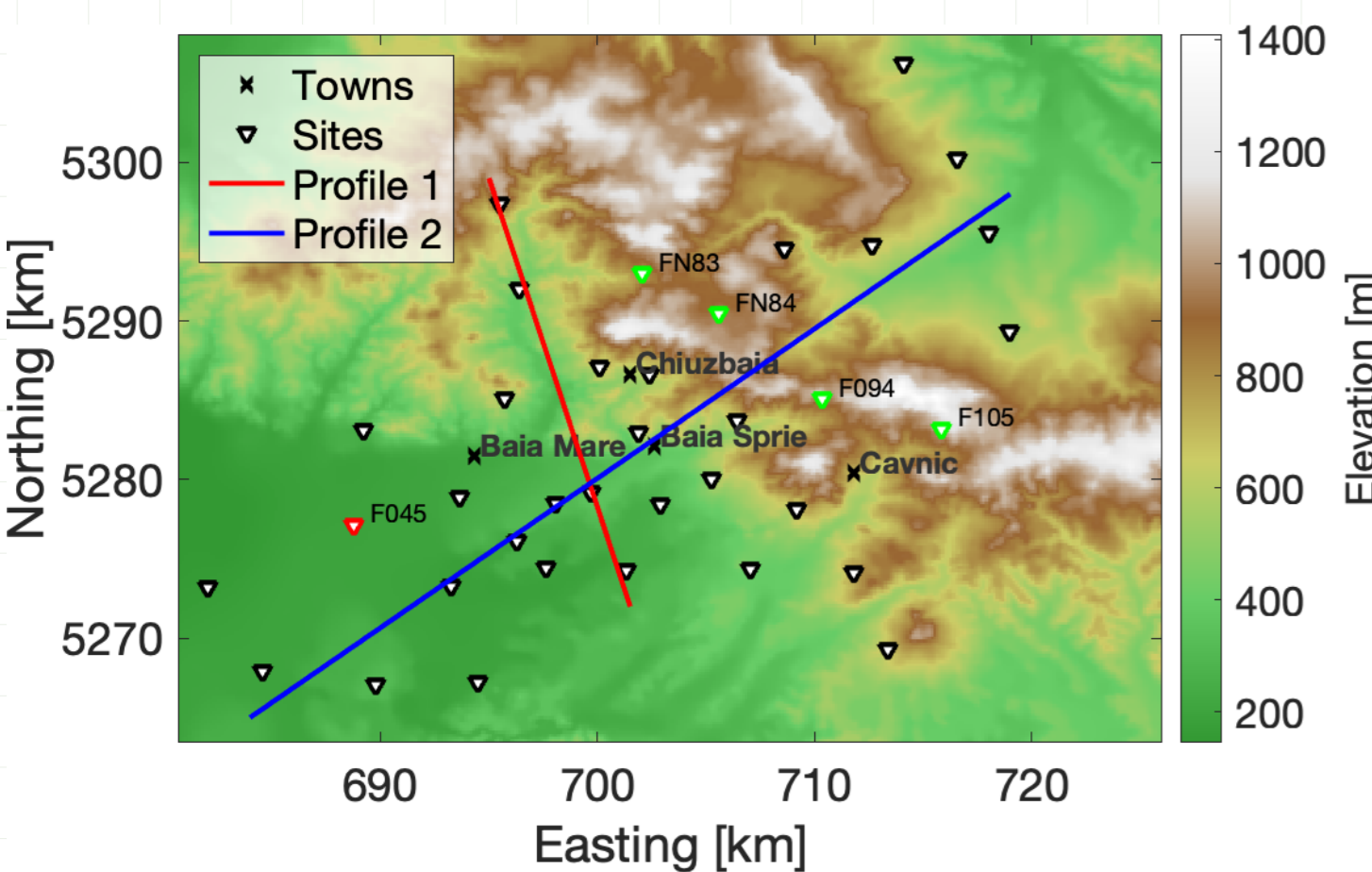


Figure 2: Topography and site locations are displayed for the study area. Sites in Figs. 3 and 5 are coloured red and green, respectively.

1 Introduction and Motivation

Galvanic distortion of the electric field [Chave et al., 2012, Jones, 2012] and topographic effects [Jiracek, 1990] pose significant challenges in 3D Magnetotelluric (MT) data interpretation. Near-surface anomalies can distort measured electric fields, leading to inaccurate subsurface models [Larsen, 1973, Berdichevsky and Dmitriev, 1976, Groom and Bailey, 1989a, Caldwell et al., 2004]. Unresolved topography further complicates forward modeling and inversion stability.

Mitigating galvanic distortion often involves advanced processing techniques or incorporating additional model parameters, adding complexity to the inversion process [Groom and Bailey, 1989a, Caldwell et al., 2004, Neukirch et al., 2019, 2020, Avdeeva et al., 2015, Moorkamp et al., 2020, Varlısüha, 2020]. Addressing topographic effects requires detailed terrain modeling to correct surface distortions [Nam et al., 2007, Usui, 2015, Käuffel et al., 2018, Soyer et al., 2019, Varlısüha, 2020].

This study assesses the impact of topography and galvanic distortion on MT data from the Northeast Carpathian Volcanic Arc [Neukirch et al., 2024] using ModEM [Kelbert et al., 2014] and DEVA3DMT [Varlısüha, 2020] inversion software. By comparing the results from these tools, we highlight their strengths and limitations in modeling subsurface conductivity in complex terrains.

2 Methods

We utilized 3D MT data from 36 sites in the Baia Mare mining area, Northern Romania, along with additional electric field measurements at 5 sites. Two data subsets were analyzed: (1) long-period data (8 Hz to 16,384 s) from 36 MT sites to evaluate distortion effects, and (2) broadband data (128 Hz to 8,192 s) from 36 MT and 5 pseudo-MT sites to assess topographic effects.

The first subset was inverted using ModEM, a finite-difference method, and DEVA3DMT, a hybrid finite element method. Inversions were performed in a flat Earth model with and without distortion correction. Data were corrected for galvanic distortion using GADGET [Neukirch et al., 2020]. The computational domain used a nonuniform grid with lateral cell dimensions of about 1 km, ModEM started with a thickness of 10 m, increasing by a factor of 1.15. DEVA3DMT used the same data and model discretization but with finer depth layering. The second subset was inverted using three approaches: 1) with ModEM and a flat Earth, 2) with ModEM and topography, and 3) with DEVA3DMT and topography. The model maintained a cell width of 1 km, but ModEM started with a cell thickness of 50 m, increasing by a factor of 1.2, while DEVA3DMT employed an adaptive mesh with a smaller initial thickness. A $30 \Omega\text{m}$ half-space served as the starting model.

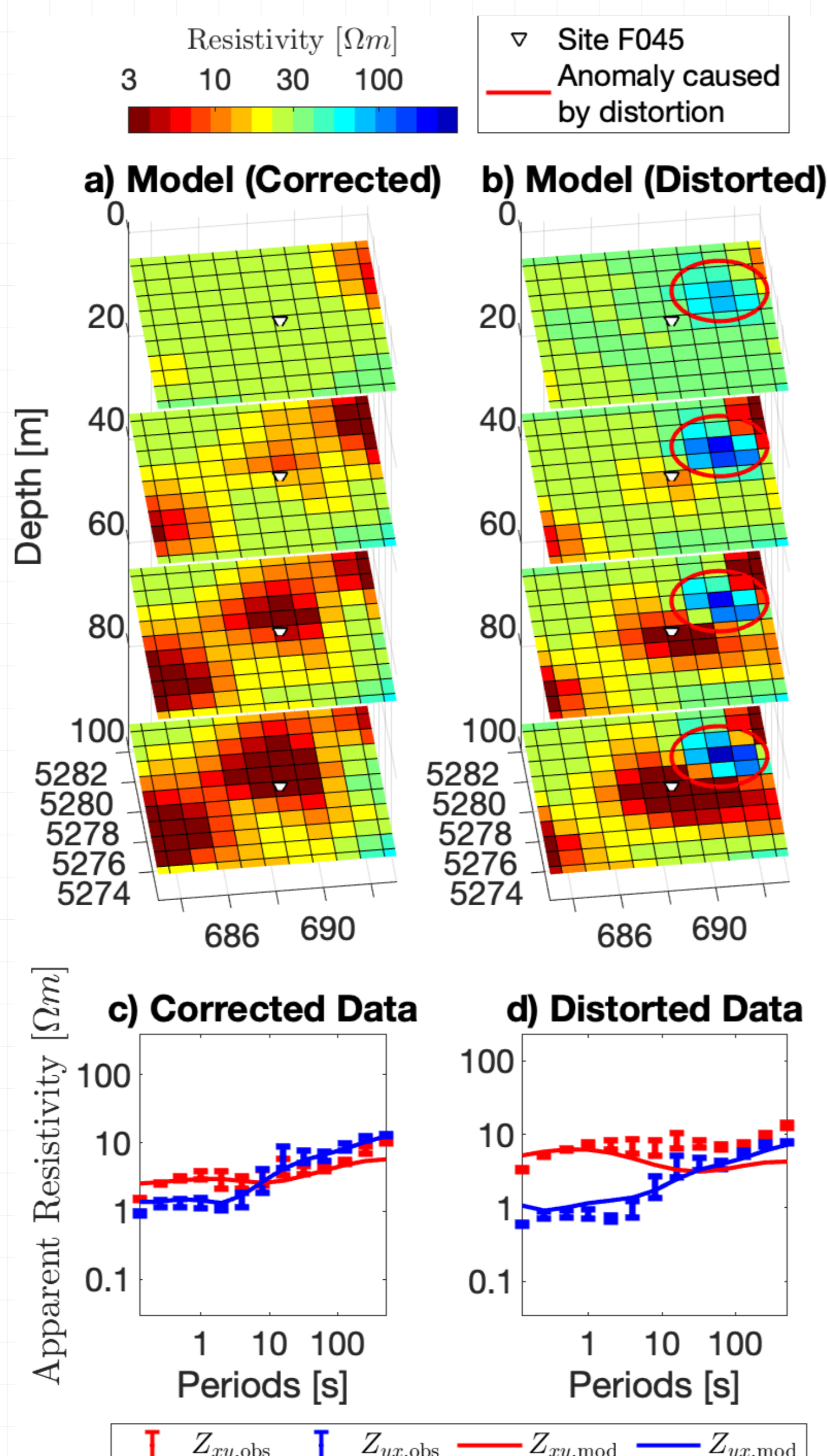


Figure 3: Inversion results of distortion-corrected and distorted data are shown. The model between 0 and 100 m below a strongly distorted MT site is illustrated (a and b) and off-diagonal apparent resistivity for observed and modelled data are compared (c and d).

3 Results and Discussion

For the entire dataset, including all sites, inverting the corrected data with ModEM resulted in a lower overall RMS error (1.53) compared to the uncorrected data (2.14). At site F045, which exhibited significant galvanic distortion (Figures 3a and b), an anomalous feature emerged in the uncorrected data inversion, likely an artifact, compromising the reliability of deeper sections as the long-period data fit was worse (Figures 3c and d). Similarly, DEVA3DMT produced a reasonably good model fit with corrected data (RMS 1.67) but struggled with distorted data (RMS 2.25) despite estimating distortion as additional parameters. A comparison of estimated distortion parameters (Figure 4) reveals notable differences, with the GADGET-corrected inversion achieving a significantly better fit.

We also compared forward-modeled responses from three inversion approaches against measured and corrected data at four sites (Figure 5). ModEM, using a flat Earth model, had an RMS error of 1.56, but its performance declined when incorporating topography due to grid coarseness (RMS = 2.92). In contrast, DEVA3DMT, which incorporates topography using the finite element method, achieved a better fit (RMS = 1.65). Refining the grid in ModEM's topography-inclusive inversion could improve results but would increase complexity, run time, and might introduce unsupported anomalies.

The models resulting from the seven different approaches are shown in top view in Figure 1 and along two profiles in Figures 6 and 7. The locations of these profiles are illustrated in Figure 2.

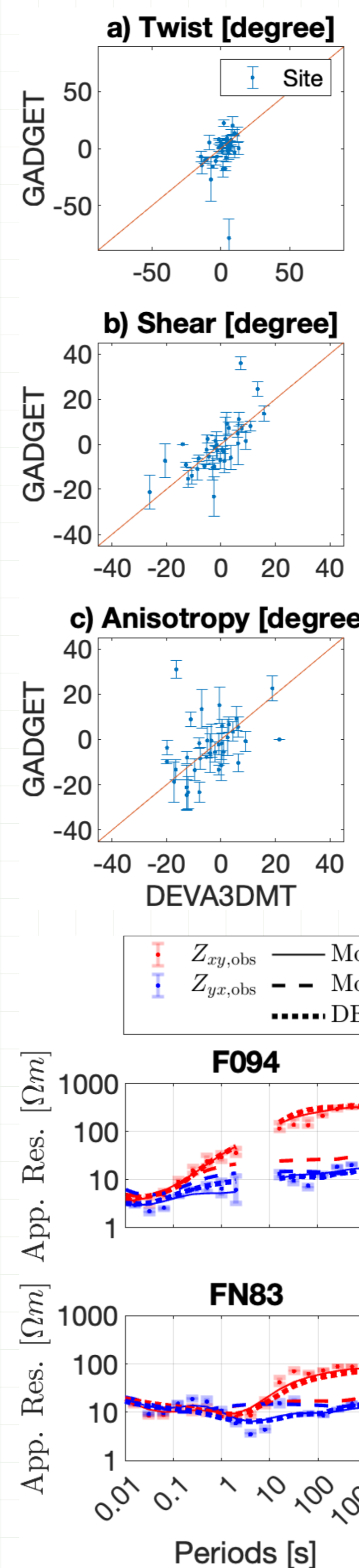


Figure 4: Estimated distortion parameters are compared between GADGET [Neukirch et al., 2020] and DEVA3DMT using the parameterization from Groom and Bailey [1989b]. GADGET (y-axis) employs a semi-analytic approach to remove galvanic distortion from each site's impedance data, while DEVA3DMT (x-axis) includes distortion parameters as model parameters during inversion. DEVA3DMT also estimates the gain, which GADGET cannot. The red line indicates equality between the estimates. Both methods yield different estimates for many sites, a result warranting further investigation.

4 Conclusion

- Challenges in interpreting 3D MT data due to topographic variations and galvanic distortion were studied using a survey in the Baia Mare mining district, Northern Romania.
- ModEM (finite-difference) performed exceptionally well assuming flat terrain, while DEVA3DMT (finite-element) effectively handled arbitrary topography.
- Distortion-corrected data yielded a lower RMS error (1.53 vs. 2.14), emphasizing the need for galvanic distortion correction.
- Galvanic distortion impacts both near-surface and deeper model sections.

Acknowledgement

We are indebted to the ModEM team for permitting the free use of their software (<https://www.modem-inversion.org>). The research leading to these results has received funding from the Norway Grants 2014-2021, under Project Contract No. 12/2020, and it was partially supported by the Research Council of Norway through its Centres of Excellence scheme, project number 332523 (PHAB).

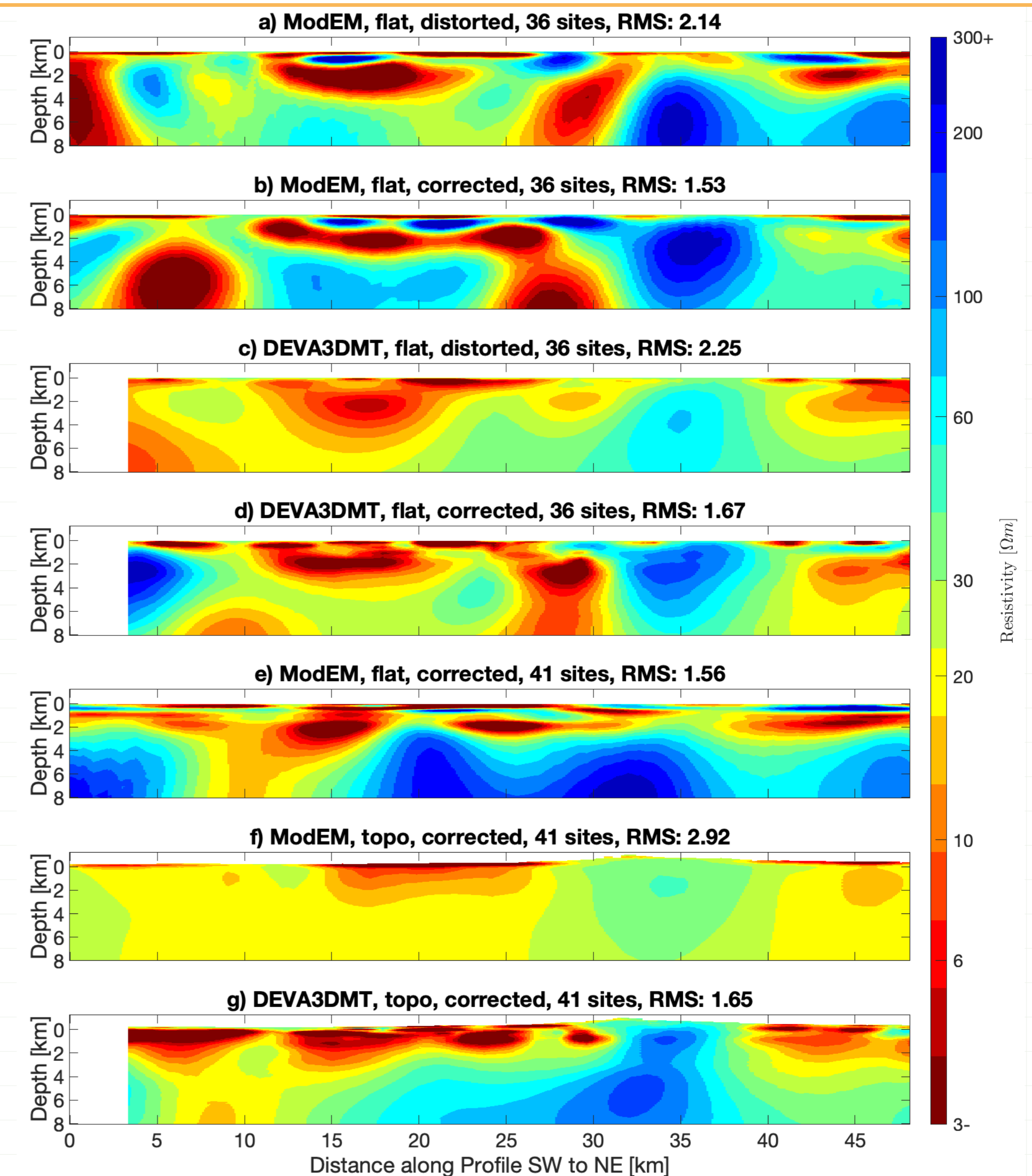


Figure 7: Resistivity models are presented along Profile 2 (see Figure 2 for location) for various inversion runs (see Figure 1 for details).

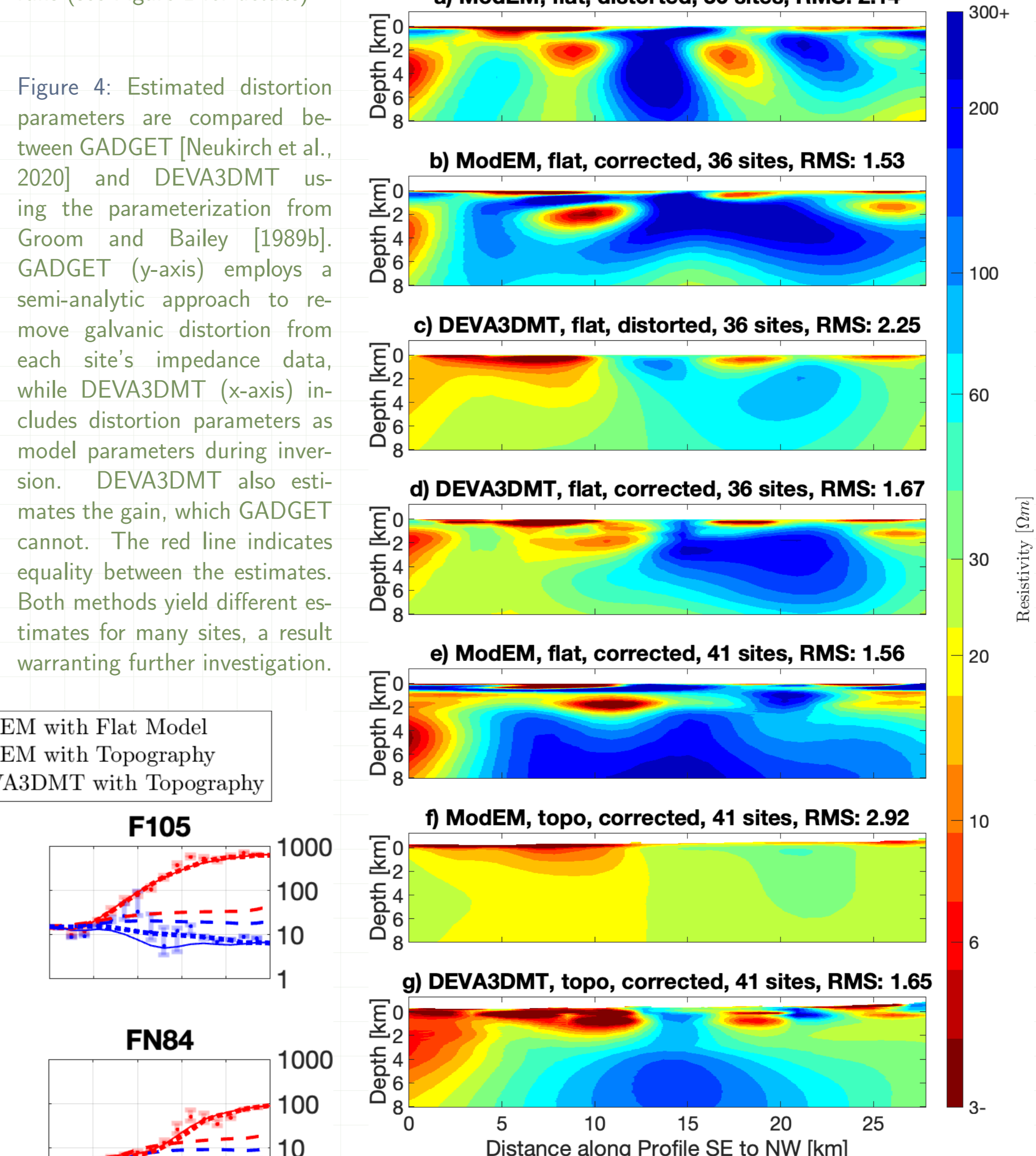


Figure 6: Resistivity models are presented along Profile 1 (see Figure 2 for location) for various inversion runs (see Figure 1 for details).

References

A. Avdeeva, M. Moorkamp, D. Avdeev, M. Jegen, and M. Miensopust. Three-dimensional inversion of magnetotelluric impedance tensor data and full distortion matrix. *Geophysical Journal International*, 202(1):464–481, 2015.

M. N. Berdichevsky and V. I. Dmitriev. Distortion of magnetic and electric fields by near-surface lateral inhomogeneities. *Acta Geod. Geophys. Montan. Acad. Sci. Hung.*, 11:447–483, 1976.

T. G. Caldwell, H. M. Bibby, and C. Brown. The magnetotelluric phase tensor. *Geophysical Journal International*, 158(2):457–469, 2004. doi: 10.1111/j.1365-246X.2004.02281.x.

A. D. Chave, P. Weidelt, and A. G. Jones. The theoretical basis for electromagnetic induction. *AD Chave, & AG Jones, The Magnetotelluric Method*, pages 19–44, 2012.

R. W. Groom and R. C. Bailey. Decomposition of Magnetotelluric Impedance Tensors in the Presence of Local Three-Dimensional Galvanic Distortion. *Journal of Geophysical Research*, 94(B2):1913–1925, 1989a.

R. W. Groom and R. C. Bailey. Decomposition of magnetotelluric impedance tensors in the presence of local three-dimensional galvanic distortion. *Journal of Geophysical Research: Solid Earth*, 94(B2):1913–1925, 1989b.

G. R. Jiracek. Near-surface and topographic distortions in electromagnetic induction. *Surveys in geophysics*, 11(2):163–203, 1990.

A. G. Jones. Distortion of magnetotelluric data: its identification and removal. *The magnetotelluric method: Theory and practice*, page 219, 2012.

J. S. Käuffel, A. V. Grayver, and A. V. Kuvshinov. Topographic distortions of magnetotelluric transfer functions: a high-resolution 3-d modelling study using real elevation data. *Geophysical Journal International*, 215(3):1943–1961, 2018.

A. Kelbert, N. Meqbel, G. D. Egbert, and K. Tandon. Modem: A modular system for inversion of electromagnetic geophysical data. *Computers & Geosciences*, 66:40–53, 2014.

J. Larsen. An introduction to electromagnetic induction in the ocean. *Physics of the Earth and Planetary Interiors*, 1973.

M. Moorkamp, A. Avdeeva, A. T. Basokur, and E. Erdogan. Inverting magnetotelluric data with distortion correction-stability, uniqueness and trade-off with model structure. *Geophysical Journal International*, 222(3):1620–1638, 2020.

M. J. Nam, H. J. Kim, Y. Song, T. J. Lee, J.-S. Son, and J. H. Suh. 3d magnetotelluric modelling including surface topography. *Geophysical Prospecting*, 55(2):277–287, 2007.

M. Neukirch, D. Rudolf, X. Garcia, and S. Galiana. Amplitude-phase decomposition of the magnetotelluric impedance tensor. *Geophysics*, 84(5):E301–E310, 2019.

M. Neukirch, S. Galiana, and X. Garcia. Appraisal of magnetotelluric galvanic electric distortion by optimizing amplitude and phase tensor relations. *Geophysics*, 85(3):E79–E98, 2020.

M. Neukirch, A. Minakov, M. Smirnov, C. Gaiña, I. Munteanu, and I. Pana. Electrical resistivity imaging of the northeast carpathian volcanic arc with 3-d magnetotellurics reveals shallow hydrothermal system. *Journal of Geophysical Research: Solid Earth*, 129(7):e2023JB028230, 2024. doi: <https://doi.org/10.1029/2023JB028230>. URL <https://agupubs.onlinelibrary.wiley.com/doi/abs/10.1029/2023JB028230>. e2023JB028230 2023JB028230.

W. Soyer, F. Miorelli, and R. Mackie. Using finite dipole lengths in complete earth 3d mt modelling. *ASEG Extended Abstracts*, 2019(1):1–4, 2019. doi: 10.1080/22020586.2019.12073129.

Y. Usui. 3-d inversion of magnetotelluric data using unstructured tetrahedral elements: applicability to data affected by topography. *Geophysical Journal International*, 202(2):828–849, 2015.

D. Varlısüha. 3d inversion of magnetotelluric data by using a hybrid forward-modeling approach and mesh decoupling. *Geophysics*, 85(5):E191–E205, 2020.